# Efficient coupling and field enhancement for the nano-scale: plasmonic needle

**Alexander Normatov[1], Pavel Ginzburg[1,*], Nikolai Berkovitch[1], Gilad M. Lerman[2], Avner Yanai[2], Uriel Levy[2] and Meir Orenstein[1]**

*[1]EE department, Technion – Israel Institute of Technology, Technion City, Haifa 32000 Israel*
*[2]Department of Applied Physics, The Benin School of Engineering and Computer Science, The Center for Nanoscience and Nanotechnology, The Hebrew University of Jerusalem, Jerusalem, 91904, Israel*
**gpasha@tx.technion.ac.il*

**Abstract:** Theoretical demonstration of efficient coupling and power concentration of radially-polarized light on a conical tip of plasmonic needle is presented. The metallic needle is grown at the center of radial plasmonic grating, engraved in a metal surface. The electromagnetic field distribution was evaluated by Finite Elements and Finite-Difference-Time-Domain methods. The results show that the field on the tip of the needle is significantly enhanced compared to the field impinging on the grating. The power enhancement exhibited a resonant behavior as a function of needle length and reached values of $\sim 10^4$. Test samples for few types of characterization schemes were fabricated.

©2010 Optical Society of America

**OCIS codes:** (240.6680) Optics at surfaces: Surface plasmons; (310.6628) Subwavelength structures, nanostructures

## References and links:

1. A. Boltasseva, and V. M. Shalaev, "Fabrication of optical negative-index metamaterials: recent advances and outlook," Metamaterials (Amst.) **2**(1), 1–17 (2008).
2. A. Maier, *Plasmonics: Fundamentals and Applications*, (Springer Science + Business Media LLC, 2007).
3. A. V. Zayats, I. I. Smolyaninov, and A. A. Maradudin, "Nano-optics of surface plasmon polaritons," Phys. Rep. **408**(3-4), 131–314 (2005).
4. E. Prodan, C. Radloff, N. J. Halas, and P. Nordlander, "A hybridization model for the plasmon response of complex nanostructures," Science **302**(5644), 419–422 (2003).
5. M. I. Stockman, "Nanofocusing of Optical Energy in Tapered Plasmonic Waveguides," Phys. Rev. Lett**. 93**, 137404 (2004).
6. P. Ginzburg, D. Arbel, and M. Orenstein, "Gap plasmon polariton structure for very efficient microscale-to-nanoscale interfacing," Opt. Lett. **31**(22), 3288–3290 (2006).
7. P. Ginzburg, and M. Orenstein, "Plasmonic transmission lines: from micro to nano scale with λ/4 impedance matching," Opt. Express **15**(11), 6762–6767 (2007).
8. G. A. Wurtz, and A. V. Zayats, "Nonlinear surface plasmon polaritonic crystals," Laser Photon. Rev. **2**(3), 125–135 (2008).
9. J. B. Khurgin, G. Sun, and R. A. Soref, "Enhancement of luminescence efficiency using surface plasmon polaritons: figures of merit," J. Opt. Soc. Am. B **24**(8), 1968–1980 (2007).
10. I. Gontijo, M. Boroditsky, E. Yablonovitch, S. Keller, U. K. Mishra, and S. P. DenBaars, "Coupling of InGaN quantum-well photoluminescence to silver surface plasmons," Phys. Rev. B **60**(16), 11564–11567 (1999).
11. R. W. Ziolkowski, and N. Engheta, Metamaterials: Physics and Engineering Explorations, (IEEE Press, John Wiley & Sons, Inc.: New York, 2006).
12. R. J. Pollard, A. Murphy, W. R. Hendren, P. R. Evans, R. Atkinson, G. A. Wurtz, A. V. Zayats, and V. A. Podolskiy, "Optical nonlocalities and additional waves in epsilon-near-zero metamaterials," Phys. Rev. Lett. **102**(12), 127405 (2009).
13. C. Ropers, C. C. Neacsu, T. Elsaesser, M. Albrecht, M. B. Raschke, and C. Lienau, "Grating-coupling of surface plasmons onto metallic tips: a nanoconfined light source," Nano Lett. **7**(9), 2784–2788 (2007).
14. E. Verhagen, A. Polman, and L. K. Kuipers, "Nanofocusing in laterally tapered plasmonic waveguides," Opt. Express **16**(1), 45–57 (2008).
15. Z. Liu, J. M. Steele, W. Srituravanich, Y. Pikus, C. Sun, and X. Zhang, "Focusing surface plasmons with a plasmonic lens," Nano Lett. **5**(9), 1726–1729 (2005).
16. A. Yanai, and U. Levy, "Plasmonic focusing with a coaxial structure illuminated by radially polarized light," Opt. Express **17**(2), 924–932 (2009).

#127981 - $15.00 USD Received 4 May 2010; revised 2 Jun 2010; accepted 4 Jun 2010; published 15 Jun 2010
(C) 2010 OSA

17. G. M. Lerman, A. Yanai, and U. Levy, "Demonstration of nanofocusing by the use of plasmonic lens illuminated with radially polarized light," Nano Lett. **9**(5), 2139–2143 (2009).
18. W. Chen, D. C. Abeysinghe, R. L. Nelson, and Q. Zhan, "Plasmonic lens made of multiple concentric metallic rings under radially polarized illumination," Nano Lett. **9**(12), 4320–4325 (2009).
19. G. Rui, W. Chen, Y. Lu, P. Wang, H. Ming, and Q. Zhan, "Plasmonic near-field probe using the combination of concentric rings and conical tip under radial polarization illumination," J. Opt. **12**(3), 035004 (2010).
20. A. Normatov, N. Berkovitch, P. Ginzburg, G. M. Lerman, A. Yanai, U. Levy, and M. Orenstein, "Nano-Coupling and Enhancement in Plasmonic Conical Needle," Proceedings of the *Quantum Electronics and Laser Science Conference (QELS)* 2010, paper QThH2.
21. P. Ginzburg, A. Hayat, N. Berkovitch, and M. Orenstein, "Nonlocal ponderomotive nonlinearity in plasmonics," Opt. Lett. **35**(10), 1551–1553 (2010).
22. G. Veronis, and S. Fan, "Bends and splitters in metal-dielectric-metal subwavelength plasmonic waveguides," Appl. Phys. Lett. **87**(13), 131102 (2005).
23. E. Feigenbaum, and M. Orenstein, "Perfect 4-way splitting in nano plasmonic X-junctions," Opt. Express **15**(26), 17948–17953 (2007).
24. H. J. Lezec, A. Degiron, E. Devaux, R. A. Linke, L. Martin-Moreno, F. J. Garcia-Vidal, and T. W. Ebbesen, "Beaming light from a subwavelength aperture," Science **297**(5582), 820–822 (2002).
25. E. Feigenbaum, and M. Orenstein, "Ultrasmall volume plasmons, yet with complete retardation effects," Phys. Rev. Lett. **101**(16), 163902 (2008).
26. P. Berini, "Plasmon-polariton waves guided by thin lossy metal films of finite width: bound modes of symmetric structures," Phys. Rev. B **61**(15), 10484–10503 (2000).
27. A. F. Oskooi, D. Roundy, M. Ibanescu, P. Bermel, J. D. Joannopoulos, and S. G. Johnson, "MEEP: A flexible free-software package for electromagnetic simulations by the FDTD method," Comput. Phys. Commun. **181**(3), 687–702 (2010).

## 1. Introduction

Fast development of nano-scale technology enables the examination of basic phenomena in physics, biology and chemistry, and allows a variety of implementations and applications. Exploiting e-beam and ion-beam nano-writing techniques, it is possible to fabricate high quality noble metal nano-structures [1] and study their interaction with light. Metals, having negative electrical dielectric constant at visible and infra-red domains, support Surface Plasmons Polaritons (SPPs) [2,3] which may be guided with sub-wavelength confinement and excite modes of nanometric particles [4]. Nano-focusing of SPPs was proposed and demonstrated in a variety of configurations: adiabatic conical metal rod [5], chain of metal spheres with variable radii, tapered [6] or abrupt impedance matched metal/insulator/metal (MIM) plasmonic waveguides [7]. Guided and localized plasmons may serve to enhance nonlinearities [8] and radiation efficiency of quantum emitters [9,10]. Arrays of plasmonic nanowires may also serve as building blocks for metamaterials [11,12]. Recent experiments exhibited some merits of these focusing for 3D [13] and, mainly, on planar focusing tapers [14]. A different focusing configuration is the planar plasmonic lens, generating circular converging SPP waves from a circular aperture [15]. It was shown recently that plasmonic assisted focusing is much more efficient if the impinging light is radially polarized - better matching both the circular symmetry of the structure and the plasmon polarization. In addition it allows for constructive interference of the dominant out-of-plane electric field component at the center of the structure [16,17, and 18,].

Exploiting these ideas, two groups recently proposed independently focusing structures with some similarity [19,20]. Here we discuss in detail the configuration of Ref. [20], evaluate theoretically, design and fabricate a plasmonic structure aimed at efficient launching of radially polarized incident illumination onto a plasmonic nanowire waveguide (needle) and subsequently to the needle tip. The proposed plasmonic structure comprises radial gratings, coupling the incident illumination to SPPs and a plasmonic nanowire waveguide of finite length, terminated by a short conical tipped segment (placed in the center of the grating). Part of the excited SPP is focused towards the center of symmetry due to the radial nature of the structure. These focused SPPs are efficiently matched to excite the highly confined mode of the plasmonic needle (the anti-symmetrical mode), and further substantial intensity enhancement occurs as the light is propagating to the apex of the short cone, as predicted in [5]. This focusing structure model is illustrated schematically in Fig. 1(a). Actual devices,

#127981 - $15.00 USD Received 4 May 2010; revised 2 Jun 2010; accepted 4 Jun 2010; published 15 Jun 2010
(C) 2010 OSA

shown in Fig. 1(b), were fabricated by a two step process at the same chamber. First, the radial gratings were generated using focused ion beam (FIB) with a precise control over the grating height and period. Subsequently a gold needle with a conical tip was grown on the center by means of low current electron beam assisted local deposition of Au from gas phase precursor. A variety of device parameters were shown to be controlled: needle height and diameter (Fig. 1(b)), gratings period and modulation depth which are promising results for on-going experiments.

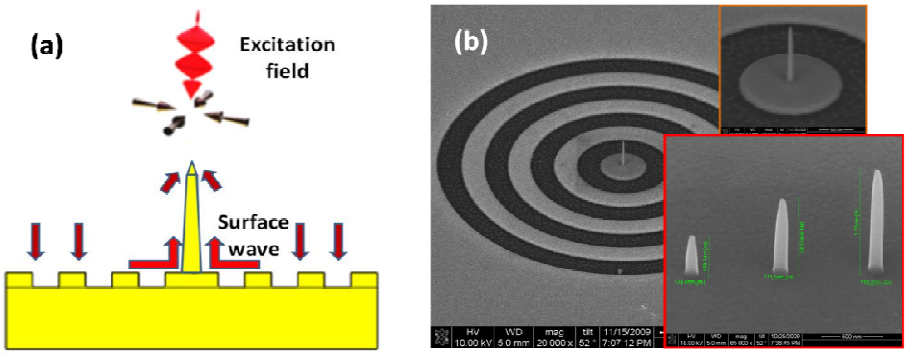


Fig. 1. (a) The schematics of the structure proposed for efficient coupling of radially-polarized light to plasmonic needle apex (b) SEM image of a fabricated device (grooves were etched here down to the substrate for visual clarity, while in the actual device they were only slightly etched); upper inset: zoom on the needle; bottom inset: variety of grown needles

The excitation of such high field intensities (hot spots) is important for validating basic limiting factors of plasmonic power concentration (e.g. nonlocal effects [21]), efficient near field inspection and writing (nanolithography, memories), and efficient coupling of nano emitters/absorbers to the far field.

Our paper dwells primarily with the coupling efficiency of a converging circular plasmonic wave into a vertical finite length nanoplasmonic wire with emphasis on this 2D-1D conversion as well as on the resonance effects due to the finite length of the wire; subsequently we deal with further field concentration into the conical tip of the wire and with issues related to fabrication and measurement strategies. A paper by G. Rui, et. al. [19] deals primarily with a transmission configuration of a Bragg planar plasmonic structure coupled to a micrometer sized cone exploring mainly the overall field concentration at the tip of the whole structure.

The analysis of the structure is done in four steps to distinguish between different enhancement mechanisms. The first is aimed at evaluation of the field enhancement of a converging circular plasmonic wave and its coupling efficiency to the needle. The second step examines the design of circular gratings aimed at efficient coupling of the incident radial illumination to SPPs. The third explores the influence of the needle height. Finally the dependence of the plasmonic modes on the excitation polarization was investigated.

## 2. Coupling of converging circular plasmonic wave to a nano needle

SPP waves were shown to be relatively robust against sharp bending scenarios even for $\pi/2$ bends [22,23]. While previous investigations dealt mainly with two-dimensional plasmonic waveguides, three-dimensional case was not fully addressed. Here we investigate the coupling efficiency of a converging, radially symmetric, circular SPP wave to nanometric diameter plasmonic needle. The needle resides in the center of symmetry vertically attached to a thick gold film, much thicker (1μm) than the penetration depth. The converging plasmonic wave is launched by applying a circular symmetric plasmonic wave source at the metal plane with transverse polarization, at the periphery of our calculation domain. At the center the in-plane plasmonic field exhibits a singularity, and the only non-vanishing electric field component is

#127981 - $15.00 USD Received 4 May 2010; revised 2 Jun 2010; accepted 4 Jun 2010; published 15 Jun 2010
(C) 2010 OSA

the one perpendicular to the surface. This latter field component – axial for the needle, leads to efficient excitation of its highly confined anti-symmetrical mode.

Calculations were performed by the Finite Element Method (FEM). The model based on circular symmetric geometry, benefits from reduction of the computation complexity and thus allows denser grid and enhanced accuracy. The device parameters were chosen in a range that matches our actual fabrication and experimental parameters. The needle height was optimized for highest local electric field enhancement at the tip. The total electric field amplitude is $|E_{tot}| = \sqrt{|E_r|^2 + |E_z|^2}$ with vanishing azimuthal component due to rotational symmetry. The resulting normalized field amplitude (in logarithmic scale) for a *965nm* high gold needle at a wavelength of 1.*55μm* is presented in Fig. 2, showing power enhancement of about $10^3$. The comparison is made for the case with no needle, where the maximum *z*-directed, field at the center is $E_{ref}$, measured just above the substrate.

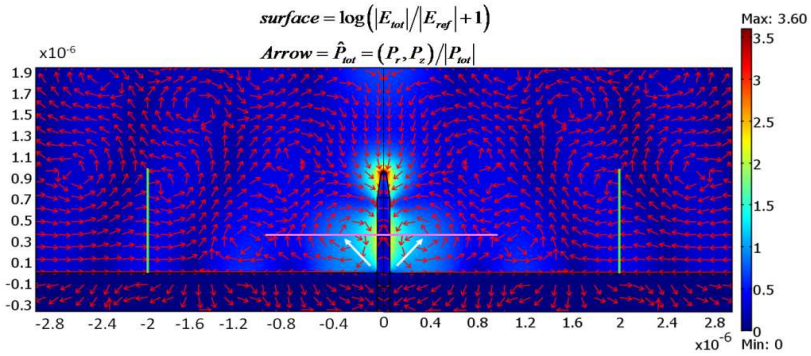


Fig. 2. Total field amplitude of a converging circular plasmonic wave on a flat gold substrate coupled to a needle. Red arrows indicate the direction of the Poynting vector.

Evaluation of SPP coupling efficiency was based on comparing the total power (*P*) flow along the substrate with the flow along the needle. The value of $P_r$ was integrated along the line $r = 2\mu m$ in the air, at the relevant heights ($0nm < z < 1\mu m$, shown as a vertical green line), yielding the substrate SPP power. The value of $P_z$ was integrated along the line $z = 350nm$ in the air, at the relevant radial distances ($55nm < r < 1.2\mu m$, shown as a horizontal pink line). The integrated power flow includes that of the needle SPP (directed downward) and the corresponding upward part of the vortex flow, centered at the position approximately indicated by the white arrows. The sum yields the non-localized portion of needle SPP power that should be compared with that of the incident substrate SPP. The resulting power coupling efficiency between the substrate surface (2D) and the needle (1D) is estimated to be >40%. The power density for the planar SPP is much smaller compared to that of the needle.

The complexity of the coupling mechanism, as it is evident from Fig. 2 implies that the coupling value can be sensitive to various surface defects within a radial range of at least one free space wavelength. These defects alter fields associated with the substrate surface SPP mode and thus may enhance or inhibit their overlap with fields associated with the needle SPP mode. The needle mode fields are defined by the needle shape which makes the shape a key parameter for the coupling. Additional numerical experiments exhibited sensitivity of field enhancement to the needle height and will be discussed below. The shape of the needle tip was defined according to that of the fabricated experimental samples. The present work does not include an investigation of the influence of the shape of the needle tip.

#127981 - $15.00 USD Received 4 May 2010; revised 2 Jun 2010; accepted 4 Jun 2010; published 15 Jun 2010
(C) 2010 OSA

## 3. Structure design for normal incidence

The parameters of the circular gratings were chosen according to a momentum matching formula for the second order resonance [16]. The design of the whole structure may be optimized for front illumination (the side with the needle), as well as for back side illumination. The first configuration is aimed for experiments where the measurements of the field concentration is indirect – e.g. by far field monitoring of nonlinear higher harmonic generation, while the second configuration is designed for direct measurement by near field scan. Here the first configuration is analyzed, while both versions were fabricated.

A circular gratings structure, similar to the structure used to harvest linearly polarized light onto a hole for enhanced transmission [24], couples the radially polarized light to converging circular plasmonic waves. The structure design that incorporates a height-optimized needle was performed for free space wavelength of *1.55μm* and is shown in Fig. 3:

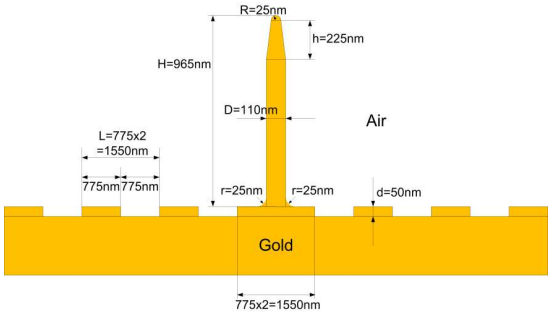


Fig. 3. The height-optimized structure design, implemented for free space wavelength of 1.55μm

The resulting normalized distribution of the real part value of the field components is depicted in Fig. 4: The $E_r$ field distribution in Fig. 4(a) shows both the standing wave pattern of the radial illumination and, in correspondence with Fig. 4(b), the vortex field distribution as was indicated in Fig. 2. It must be noted that the color-scales of Fig. 4 are fitted to accommodate representation of weaker fields remote from the needle and thus at the needle tip the field values are saturated. The $E_z$ values at the needle tip correspond to power enhancement of the order of $10^4$, as will be demonstrated in the next section. Here $E_{ref}$ is the $z$ directed field in the center of the structure when the needle is not present.

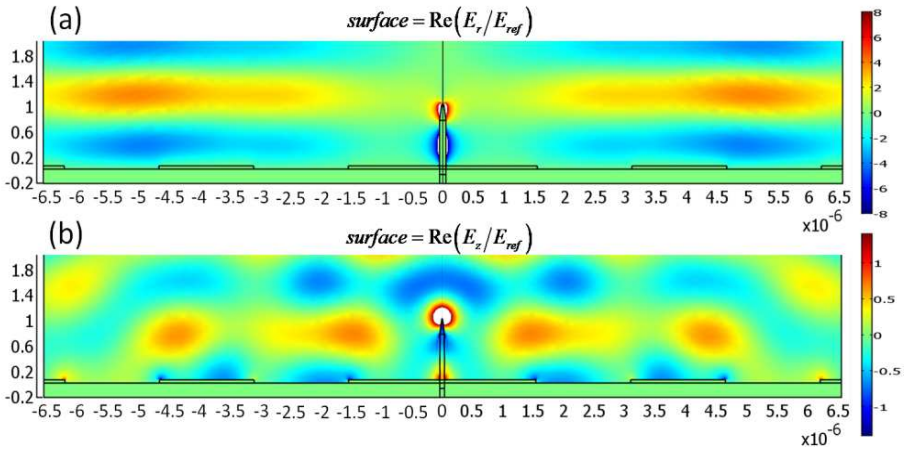


Fig. 4. Normalized value of the electric field components is shown for the height-optimized needle. (a) The $E_r$ field; (b) The $E_z$ field.

#127981 - $15.00 USD Received 4 May 2010; revised 2 Jun 2010; accepted 4 Jun 2010; published 15 Jun 2010
(C) 2010 OSA

## 4. Resonant behavior of field enhancement

The basic phenomenon, leading to the field enhancement at the tip, is the narrowing of the SPP mode when propagating to the needle tip. In contrary to the theoretical ideal adiabatic infinitely tipped cone of Ref [5], where no back reflection from the tip is expected due to SPP adiabatic stopping, the conical part of our needle is finite. Thus reflection from the apex is exhibited, depending on the specific tip shape and wavelength. In addition, the needle base is not completely impedance matched to the planar SPP structure and consequently partial refection occurs there as well. This turns the needle into a Fabry-Perot (FP) like resonator where the reflection phases are of great importance and the longitudinal modes that are supported by the FP resonators obey the following equation [25]:

$$4\pi h/\lambda_{avg} + \theta_1 + \theta_2 = 2\pi N \qquad (1)$$

where $h$ is the needle height, $\lambda_{avg}$ the averaged SPP wavelength ($\lambda$ varies along the needle according to the local diameter), and $\theta_{1,2}$ are reflection phases from the top and the bottom of the needle. This resonance can be illustrated by varying the plasmonic needle height and measuring $E_z$ field enhancement at the conical tip ($E_r$ = 0 there), relative to the field in the center of the gratings structure with no needle. The results showing the ratio of field enhancement are shown in Fig. 5. The difference in the plasmonic needle height between consecutive peaks (resonances), is about 700nm. This means that $\lambda_{avg}$, which ideally should be equal to a half of the free space wavelength, corresponds to averaged SPP effective index of *~1.1* (when the refection phases are assumed to be non-dispersive). Largest field enhancement corresponding to the investigated positive defect was about 150. Figure 6 shows the field distributions, corresponding to the peaks, represented in Fig. 5.

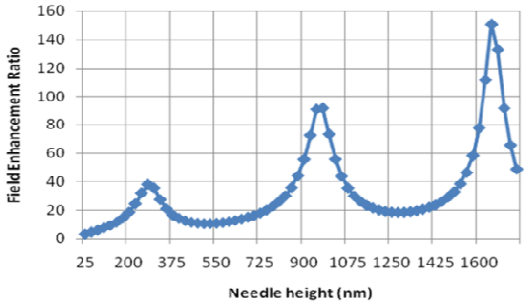


Fig. 5. $E_z$ field enhancement at the needle tip as a function of needle height for $\lambda_0$ = *1550nm*.

The absolute value of $E_{tot}$ is $|E_{tot}| = \sqrt{|E_r|^2 + |E_z|^2}$, as the incident illumination is radially polarized and the structure has cylindrical symmetry.

#127981 - $15.00 USD Received 4 May 2010; revised 2 Jun 2010; accepted 4 Jun 2010; published 15 Jun 2010
(C) 2010 OSA

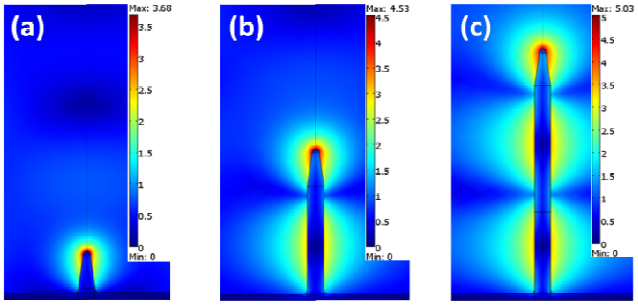


Fig. 6. Field distribution cross section corresponding to the local maxima of Fig. 5. For visualization, the relative field values are shown as $\log(|E_{tot}|/|E_{ref}| + 1)$ (a) at 300nm (b) at 950nm (c) at 1670nm.

Figure 6(a) confirms that at the first (electrostatic) resonance of the structure the needle height is small compared to the excitation wavelength. Figures 6(b), (c) show the second and third structure resonances or first and second cavity (retarded) resonances. Additional optimizations may further enhance the field.

## 5. Needle modes and their dependence on impinging polarization

The nano needle supports two bound modes with symmetric and antisymmetric profiles [26]. The mode with antisymmetric magnetic field profile is the mode of interest here since it has the highly confined field. Radial polarization illumination exhibits an antisymmetric field component ($H_\varphi$) around the center, matching the required needle excitation. On the other hand, linear (circular) polarization excites the symmetric and much less confined mode.

Differences in confinement between these two excitation polarizations are calculated by Finite Difference Time Domain method [27] and shown in Fig. 7. Comparing Fig. 7(a) - two Fabry Perot lobes, and 7(c) - three Fabry Perot lobes, reveals that the effective wavelength at the tip is much smaller under radial polarization illumination – as expected by the confined mode dispersion. Also, the much higher confinement is evident. Comparison between Fig. 7 (b) and (c) shows that only for radial polarization the strong $E_Z$ component (along the tip) resides at the tip.

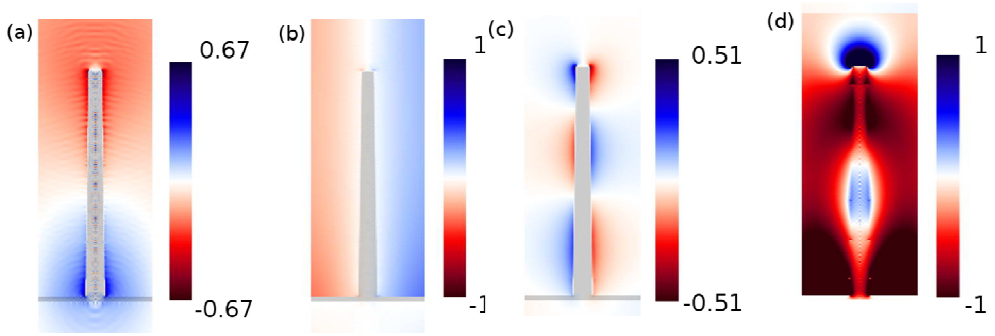


Fig. 7. Field distribution for 950nm high tip. (a) transverse field excited by linear polarization illumination (b) longitudinal field obtained by linear polarization illumination (c) transverse field by radial polarization illumination (d) longitudinal field by radial polarization illumination. The color scaling of (b) and (d) is normalized and for (a) and (c) is proportional to (b) and (d) respectively.

## 6. Outlook and conclusions

On-going measurements are aimed at the evaluation of the field enhancement as a function of excitation wavelength, polarization and design parameters. The resonant sensitivity of the

#127981 - $15.00 USD Received 4 May 2010; revised 2 Jun 2010; accepted 4 Jun 2010; published 15 Jun 2010
(C) 2010 OSA

structure, as discussed above, (significant enhancement for restricted wavelength / needle length combinations) will be employed to eliminate the background of the non enhanced fields. The enhanced Au based second harmonic generation by a pulsed excitation at *1.5μm* and *0.85μm* regimes and the actual field distributions will be measured by NSOM.

In conclusion, we propose a configuration of a nanometric plasmonic needle, surrounded by a radial gratings, yielding power enhancement factor of the order of $10^4$. The fabricated samples are currently under measurements. High coupling efficiency of this structure to single quantum emitters may open possibilities to realize quantum memories and quantum gates in the near future. The high field concentration at the nano-scale opens possibilities to test basic nonlinear properties of isolated nano-structures.

#127981 - $15.00 USD Received 4 May 2010; revised 2 Jun 2010; accepted 4 Jun 2010; published 15 Jun 2010
(C) 2010 OSA